Search Strategy for Sleptons and Dark Matter Using the LHC as a Photon Collider

Lydia Beresford* and Jesse Liu†
Department of Physics, University of Oxford, Oxford OX1 3RH, United Kingdom

(Received 3 December 2018; revised manuscript received 22 July 2019; published 3 October 2019)

We propose a search strategy using the LHC as a photon collider to open sensitivity to scalar lepton (slepton $\tilde{\ell}$) production with masses around 15 to 60 GeV above that of neutralino dark matter $\tilde{\chi}_1^0$. This region is favored by relic abundance and muon $(g-2)_\mu$ arguments. However, conventional searches are hindered by the irreducible diboson background. We overcome this obstruction by measuring initial state kinematics and the missing momentum four-vector in proton-tagged ultraperipheral collisions using forward detectors. We demonstrate sensitivity beyond LEP for slepton masses of up to 200 GeV for $15 \lesssim \Delta m(\tilde{\ell}, \tilde{\chi}_1^0) \lesssim 60$ GeV with 100 fb^{-1} of 13 TeV proton collisions. We encourage the LHC collaborations to open this forward frontier for discovering new physics.

DOI: 10.1103/PhysRevLett.123.141801

Introduction.—Elucidating the elementary properties of dark matter (DM) is among the most urgent problems in fundamental physics. The lightest neutralino $\tilde{\chi}_1^0$ in supersymmetric (SUSY) extensions of the standard model (SM) is one of the most motivating DM candidates [1–3]. A favored scenario involves scalar partners of the charged leptons (sleptons $\tilde{\ell}$) being 1 to tens of GeV above the $\tilde{\chi}_1^0$ mass. This enables interactions that reduce the $\tilde{\chi}_1^0$ cosmological relic abundance to match the observed value [4] via a mechanism called slepton coannihilation [5,6]. Furthermore, partners of the muon (smuon $\tilde{\mu}$) and neutralinos with masses near the weak scale are a leading explanation for 3σ to 4σ deviations between measurements of the muon magnetic moment and SM prediction [7–10].

Remarkably, Large Hadron Collider (LHC) searches for these key targets have no sensitivity when mass differences are $15 \lesssim \Delta m(\tilde{\ell}, \tilde{\chi}_1^0) \lesssim 60$ GeV [11–14]. Here, Large Electron Positron (LEP) collider limits remain the most stringent, excluding $m(\tilde{\ell}) \lesssim 97$ GeV [15–17]. Sensitivity is hindered by an obstruction generic to all LHC search strategies for invisible DM states and their mediators [18–32]: the kinematics of colliding quarks and gluons are immeasurable. Without this initial state information, the missing momentum four-vector p_{miss} left by DM can be determined only in the plane transverse to the beam ($\mathbf{p}_T^{\text{miss}}$). This precludes direct DM mass reconstruction that would otherwise provide effective discrimination against neutrino ν backgrounds.

This Letter proposes a search strategy to resolve these long-standing problems by using the LHC as a photon collider [33]. In a beam crossing, protons can undergo an ultraperipheral collision (UPC), where photons from the electromagnetic fields interact to produce sleptons exclusively, $pp \to p(\gamma\gamma \to \tilde{\ell}\tilde{\ell})p$. The sleptons decay as $\tilde{\ell} \to \ell\tilde{\chi}_1^0$, resulting in the very clean final state $p(2\ell + p_{\text{miss}})p$ of our search: two intact protons, two leptons ℓ, and missing momentum (Fig. 1). As the beam energy is known, measuring the outgoing proton kinematics determines the colliding photon momenta and thus p_{miss}. This experimental possibility is opened by the ATLAS Forward Proton (AFP) [34] and CMS-TOTEM Precision Proton Spectrometer (CT-PPS) [35,36] forward detectors, which recorded their first data in 2017 and 2016, respectively. CMS-TOTEM moreover observed double lepton production in high-luminosity proton-tagged events [37], demonstrating that initial state reconstruction is feasible.

Photon collisions at the LHC reach sufficient rates to probe rare processes such as SM light-by-light scattering [38,39], anomalous gauge couplings [40,41], axionlike particles [42,43], and dark sectors [44,45]. Nonetheless,

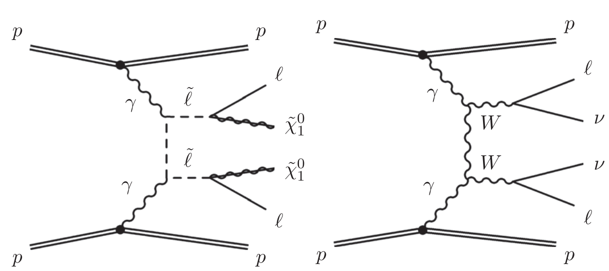

FIG. 1. Exclusive pair production of (left panel) scalar leptons ("sleptons") $\tilde{\ell}$ decaying to dark matter $\tilde{\chi}_1^0$ and (right panel) SM diboson WW background using the LHC as a photon collider.

Published by the American Physical Society under the terms of the Creative Commons Attribution 4.0 International license. Further distribution of this work must maintain attribution to the author(s) and the published article's title, journal citation, and DOI. Funded by SCOAP³.

it is widely considered that photon fusion production of sleptons is not competitive as a discovery window compared to electroweak production [11–14]; existing photon collider studies therefore focus on slepton mass measurement for specific benchmark points [46–50]. Our proposal argues to the contrary that photon collisions play an essential role in SUSY and DM searches. We emulate AFP and CT-PPS proton tagging, which enables powerful background suppression. We demonstrate a strategy that surpasses LEP sensitivity in the favored $15 \lesssim \Delta m(\tilde{\ell}, \tilde{\chi}_1^0) \lesssim 60$ GeV corridor, underscoring the importance of initial state kinematics and p_{miss} for the LHC discovery program.

Photon collider simulation.—Electromagnetic fields surrounding ultrarelativistic protons can be modeled as a beam of nearly on-shell photons, which is known as the equivalent photon approximation [51]. We consider pair production of electrically charged particles X via photon fusion $\gamma\gamma \to XX$. Analytic expressions of their QED cross sections $\sigma_{\gamma\gamma\to XX}$ may be found in Refs. [46,50,52,53]. The LHC cross section $\sigma^{(pp)}_{\gamma\gamma\to XX}$ is then the convolution of $\sigma_{\gamma\gamma\to XX}$ with the effective photon luminosity $L^{(pp)}_{\gamma\gamma}$ from the protons

$$\sigma^{(pp)}_{\gamma\gamma\to XX} = \int \sigma_{\gamma\gamma\to XX}(m_{\gamma\gamma}) \frac{dL^{(pp)}_{\gamma\gamma}}{dm_{\gamma\gamma}} dm_{\gamma\gamma}, \tag{1}$$

where $m_{\gamma\gamma}$ is the invariant mass of the two-photon system. We use MadGraph v2.6.1 [54,55] to numerically evaluate Eq. (1) and perform Monte Carlo simulations for signal and background processes. Throughout, cross sections $\sigma^{(pp)}_{\gamma\gamma\to XX}$ refer to $pp \to p(\gamma\gamma \to XX)p$ processes with default generator preselections applied, except that the lepton p_T requirement is removed. We study the resulting events using the PYLHE package [56] and parametrize the detector effects as follows.

The forward detectors identify both the intact outgoing protons at $z \simeq \pm 220$ m downstream from the collision point and measure their energies E_{forward}. Protons are steered outside the beam profile by the LHC dipole magnets due to the fractional energy loss $\xi = 1 - E_{\mathrm{forward}}/E_{\mathrm{beam}}$ relative to the beam energy $E_{\mathrm{beam}} = 6.5$ TeV. The AFP and CT-PPS proton acceptance is close to 100% for $0.02 < \xi < 0.12$ [34–36], which we emulate by requiring emitted photon energies $130 < E_\gamma < 780$ GeV. The Supplemental Material [57] validates the finding that the proton p_T is very small, which is neglected in MadGraph, and also shows the impact of raising the minimum ξ to 0.025 ($E_\gamma > 162.5$ GeV). Existing studies typically assume 100% survival probability $P^{(pp)}_{\mathrm{survival}}$ of a proton remaining intact following photon emission [46–50], but phenomenological studies suggest lower values for the range of E_γ considered [58,59]. We estimate $P^{(pp)}_{\mathrm{survival}}$ using SuperChic 3.02 [60], which we treat as an efficiency parametrized by $P^{(pp)}_{\mathrm{survival}} = a \exp(-b m_{\gamma\gamma})$, where $a = 0.988$, $b = 4.67 \times 10^{-4}$; see the Supplemental Material [57] for the origin of this parametrization. This gives $P^{(pp)}_{\mathrm{survival}} = 94\%$ for $m_{\gamma\gamma} = 100$ GeV and falls to 62% for $m_{\gamma\gamma} = 1000$ GeV. We conservatively smear the photon four-vector $p_\gamma^{\mathrm{smeared}} = p_\gamma^{\mathrm{generated}} G_\gamma(1, \sigma_\gamma)$ using a Gaussian G_γ with width $\sigma_\gamma = 5\%$, based on the AFP resolution of 5 GeV at $\xi \simeq 0.02$ [34].

The central detectors reconstruct isolated leptons (electrons e and muons μ throughout). To emulate detector resolution, we smear the lepton momenta p_ℓ using a Gaussian G_ℓ with p_T-dependent width $\sigma_\ell(p_T)$. We extract σ_ℓ from Refs. [61,62], which are predominantly below 5% for the relevant range of p_T and have minimal impact on the results. We parametrize p_T-dependent reconstruction efficiencies in accord with ATLAS [14], which accounts for all lepton quality conditions. This requires that leptons satisfy transverse momentum $p_T^{e(\mu)} > 4.5(4)$ GeV and pseudorapidity $|\eta_\ell| < 2.5$.

To simulate the simplified model signal $\gamma\gamma \to \tilde{\ell}\tilde{\ell}$, we employ the model specified by the SUSY Les Houches Accord parameter file from the auxiliary material of Ref. [14]. This allows comparisons with existing LHC constraints. Only sleptons $\tilde{\ell}$ and the stable neutralino $\tilde{\chi}_1^0$, whose masses are free parameters, are kinematically accessible. A fourfold mass degeneracy is assumed such that scalar partners of the left-handed and right-handed electrons and muons (selectrons $\tilde{e}$ and smuons $\tilde{\mu}$) satisfy $m(\tilde{\ell}_{L,R}) = m(\tilde{e}_L) = m(\tilde{e}_R) = m(\tilde{\mu}_L) = m(\tilde{\mu}_R)$. The sleptons decay $\tilde{\ell} \to \ell\tilde{\chi}_1^0$ with 100% branching ratio and are handled by MadGraph. All other SUSY states are kinematically inaccessible with masses well above 10 TeV. We sample $m(\tilde{\ell})$ in 25 GeV steps, and $\Delta m(\tilde{\ell}, \tilde{\chi}_1^0)$ in steps of no more than 20 GeV. We simulate 50×10^3 events per mass point and normalize to cross sections calculated in MadGraph, which are consistent with those obtained in Refs. [49,50]. For $m(\tilde{\ell}) = 100$ GeV, the cross section $\sigma^{(pp)}_{\gamma\gamma\to\tilde{\ell}\tilde{\ell}}$ is 2.5 fb and falls to 0.25 fb for $m(\tilde{\ell}) = 200$ GeV. Only the first two generations $\tilde{\ell} \in [\tilde{e}, \tilde{\mu}]$ are considered; study of scalar partners of τ leptons (staus $\tilde{\tau}$) are deferred to future work.

Search strategy.—Our search strategy focuses on extracting the signal from the dominant irreducible $\gamma\gamma \to WW \to \ell\nu\ell\nu$ background. The WW cross section times the dileptonic branching fraction $\mathcal{B}$ is $\sigma^{(pp)}_{\gamma\gamma\to WW} \times \mathcal{B} \simeq 5$ fb, which is comparable in size to the slepton signals. We generate 50×10^3 events of this process using MadGraph, which also handles the decays to preserve spin correlations of the leptons. We use dilepton triggers for event selection, which we emulate using a $p_T^\ell > 15$ GeV condition. Requiring same flavor leptons (ee or $\mu\mu$) halves the WW background while preserving signal. We then reconstruct three defining features that characterize the signals and background to optimize search sensitivity: mediator mass (W or $\tilde{\ell}$), invisible mass (ν or $\tilde{\chi}_1^0$), and mediator spin.

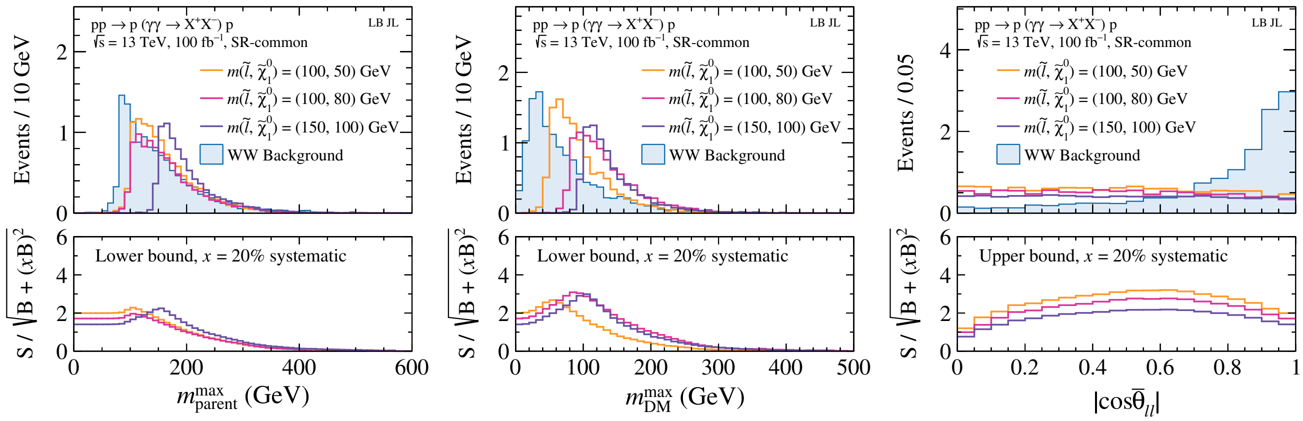

FIG. 2. Kinematic distributions of discriminants reconstructing the mass and spin for benchmark slepton signals (lines) and WW background (filled areas), normalized to 100 fb^{-1}. Proton survival, ξ acceptance, lepton efficiencies, and detector smearing are applied, but no lepton trigger emulation is imposed. The event selection applied, denoted SR-common, requires $m_{\mathrm{DM}}^{\max} > 0$ GeV, $|\eta_\ell| < 2.5$, same flavor leptons, and $m_{T2}^0 > 2$ GeV. The legend displays signal masses. The lower panels estimate the statistical significance after integrating the signal S and background B counts with the indicated bound on the variable.

At the LHC, proton tagging enables unambiguous bounds on both the parent mediator and DM masses. The mass of the $\tilde{\ell}$ mediators is bound by the invariant mass of the initial state two-photon system $m_{\gamma\gamma}^2 = (p_{\gamma_1} + p_{\gamma_2})^2 \geq (2m_{\tilde{\ell}})^2$. The Supplemental Material [57] shows that signals have broad tails in $m_{\gamma\gamma}$, allowing AFP and CT-PPS acceptance even for low masses $m(\tilde{\ell}) \lesssim 150$ GeV. Meanwhile, the invariant mass of the invisible system W_{miss} bounds the DM masses $W_{\mathrm{miss}}^2 = p_{\mathrm{miss}}^2 \geq (2m_{\tilde{\chi}_1^0})^2$. Here, $p_{\mathrm{miss}} = \sum_i p_i - \sum_f p_f$ is the vectorial sum of the momenta of the visible final states p_f subtracted from the initial states p_i. In this search, we have $\sum_i p_i = p_{\gamma_1} + p_{\gamma_2}$ and $\sum_f p_f = p_{\ell_1} + p_{\ell_2}$. We find the ratio $m_{\gamma\gamma}/W_{\mathrm{miss}}$ to be useful for $\Delta m(\tilde{\ell}, \tilde{\chi}_1^0) \lesssim 30$ GeV signals.

To improve mass reconstruction of the parent mediator and DM states, one can impose hypotheses about the decay topology. Assuming the symmetric pair of semi-invisible decays $\tilde{\ell}\tilde{\ell} \to \ell\tilde{\chi}_1^0\ell\tilde{\chi}_1^0$, with photon and lepton momenta measured, results in the Harland-Lang–Kom–Sakurai–Stirling variables defined in Ref. [50]. These also provide mass bounds on the parent mediator $m_{\mathrm{parent}}^{\max} \geq m(\tilde{\ell})$ and invisible system $m_{\mathrm{DM}}^{\max} \geq m(\tilde{\chi}_1^0)$. Importantly, these variables have more steeply falling tails than $m_{\gamma\gamma}$ and W_{miss}, respectively, and therefore provide better signal separation from the WW background.

To exploit the mediator spin, we use the Barr-Melia variable [63,64] defined by $\cos\bar{\theta}_{\ell\ell} = \tanh[\frac{1}{2}(\bar{\eta}_{\ell_1} - \bar{\eta}_{\ell_2})]$, where the pseudorapidities $\bar{\eta}$ are evaluated in the dilepton center-of-mass frame (denoted by overlines). Leptons from spin 0 $\tilde{\ell}$ mediators decay more centrally than those from spin 1 W bosons, offering discrimination power.

Figure 2 displays distributions of benchmark signals and the WW background for these mass and spin sensitive variables, normalized to 100 fb^{-1}. From this, we impose $|\cos\bar{\theta}_{\ell\ell}| < 0.65$ and construct three signal region (SR) categories targeting small "compressed," medium "corridor," and large mass differences $\Delta m(\tilde{\ell}, \tilde{\chi}_1^0)$: (1) SR-compressed—$m_{\mathrm{parent}}^{\max} > 80$ GeV, $m_{\mathrm{DM}}^{\max} > 0$ GeV, $m_{\gamma\gamma}/W_{\mathrm{miss}} < 1.5$; (2) SR-corridor—$m_{\mathrm{parent}}^{\max} > 120$ GeV, $m_{\mathrm{DM}}^{\max} > 80$ GeV; and (3) SR-large—$m_{\mathrm{parent}}^{\max} > 130$ GeV, $m_{\mathrm{DM}}^{\max} > 20$ GeV. An improved strategy would involve a shape analysis of $(m_{\mathrm{parent}}^{\max}, m_{\mathrm{DM}}^{\max})$ akin to a bump hunt [29] in two dimensions, but it is deferred to future work.

Other potential irreducible processes include $\tau\tau \to \ell\nu\nu\ell\nu\nu$, which has a large rate $\sigma_{\gamma\gamma\to\tau\tau}^{(pp)} \times \mathcal{B} \simeq 74 \times 0.35^2 \simeq 9.1$ pb. We reject this process by reconstructing the τ mass end point using the stransverse mass $m_{T2}^{\chi=0} > 2$ GeV (see Refs. [65–67] for a definition). This variable uses the lepton momenta and missing transverse momentum defined by $\mathbf{p}_T^{\mathrm{miss}} \equiv -\mathbf{p}_T^{\ell_1} - \mathbf{p}_T^{\ell_2}$. As we use this variable to reject τ's decaying to massless neutrinos, we set the hypothesized mass of the invisible state $\chi = 0$ GeV in $m_{T2}^{\chi=0}$ throughout. We validate mitigation of this background by generating an event sample in MadGraph using the `sm-lepton_masses` model to decay the τ's. The Supplemental Material [57] shows that this requirement has a signal efficiency above 95% for the target mass points $\Delta m(\tilde{\ell}, \tilde{\chi}_1^0) \gtrsim 20$ GeV. Top quark pairs $\gamma\gamma \to t\bar{t} \to b\ell\nu b\ell\nu$ contribute a small rate $\sigma_{\gamma\gamma\to t\bar{t}}^{(pp)} \times \mathcal{B} \simeq 0.33 \times 0.21^2 \simeq 0.015$ fb, and we assume that a jet veto renders this background negligible.

Turning to reducible backgrounds induced by detector misreconstruction, these typically require data driven techniques to estimate reliably. We briefly discuss possible mitigation strategies. First, nonresonant lepton pairs $\gamma\gamma \to \ell\ell$, where $\ell \in [e, \mu]$, have a large cross section $\sigma_{\gamma\gamma\to ee}^{(pp)} = \sigma_{\gamma\gamma\to\mu\mu}^{(pp)} = 60$ pb. Missing momentum results solely from detector resolution, and this background is also rendered negligible by the m_{T2} requirement. This also suppresses resonant dilepton decays of quarkonia such as J/ψ and Υ states. Next, fake and nonprompt leptons, such as semileptonic decays of B hadrons, typically become significant at low lepton p_T [14]. We expect these to be well controlled by standard lepton quality requirements. Indeed fake leptons are negligible in current slepton searches using lepton triggers [11–13].

Finally, pileup collisions can fake intact UPC protons when occurring in the same event as an exclusive or nonexclusive process with two leptons and p_{miss}. Robustly estimating these pileup backgrounds requires data driven methods. We suggest mitigation strategies for dedicated study in the experimental collaborations, with further discussion given in the Supplemental Material [57]. To suppress nonexclusive processes, recent analyses veto tracks within 1 mm of the dilepton vertex [68–70]. This can be optimized further, such as by lowering track p_T thresholds down to 100 MeV [39]. Requiring low activity in the zero degree calorimeters [71] could also suppress nonexclusive processes, with ongoing developments of radiation hard technologies for high-luminosity runs [72]. Measuring arrival time differences of forward protons with target resolutions of 10 ps [73–76] allows us to match with lepton vertices. Assuming a conservative 30 ps resolution, Ref. [76] finds a 1 order of magnitude background rejection for 90% signal efficiency, while early measurements using LHC run 2 data already reach 20 ps [77]. Further requirements could enhance signal discrimination, such as imposing low p_T forward protons, and correlating lepton and proton kinematics using multivariate techniques.

Sensitivity and discussion.—We now evaluate the sensitivity of our search strategy for the slepton-DM simplified model. We assume two benchmark luminosities $\mathcal{L} = 100\,(300)$ fb^{-1}, which correspond to the cumulative dataset for LHC run 2 (3). We use the asymptotic Poisson significance with uncertain background $Z_A(S, B, \sigma_B)$ [78,79]. This takes as input the signal S, background B counts, and we ascribe a background systematic uncertainty of $\sigma_B = 0.2B$. For 100 fb^{-1}, SR compressed has $B = 0.47$, and the highest $S = 5$ is for the $m(\tilde{\ell}, \tilde{\chi}_1^0) = (100, 80)$ GeV signal. This corresponds to a signal efficiency of 2% with respect to the generated cross section, and a significance of 3.3σ, rising to 5.7σ for 300 fb^{-1}. Meanwhile, SR corridor targets slightly larger $\Delta m(\tilde{\ell}, \tilde{\chi}_1^0)$, where $B = 0.74$ and the highest $S = 5.5$ corresponds to the $m(\tilde{\ell}, \tilde{\chi}_1^0) = (125, 80)$ GeV signal, translating to 3.3σ significance, rising to 5.7σ for 300 fb^{-1}. SR large probes larger $\Delta m(\tilde{\ell}, \tilde{\chi}_1^0)$, with $B = 1.2$ at 100 fb^{-1} and the highest $S = 5.9$ is for the $m(\tilde{\ell}, \tilde{\chi}_1^0) = (125, 40)$ GeV signal, corresponding to a significance of 3.1σ, rising to 5.4σ for 300 fb^{-1}. The Supplemental Material [57] presents cutflows showing the yields for benchmark signals and the WW background sequentially after each requirement.

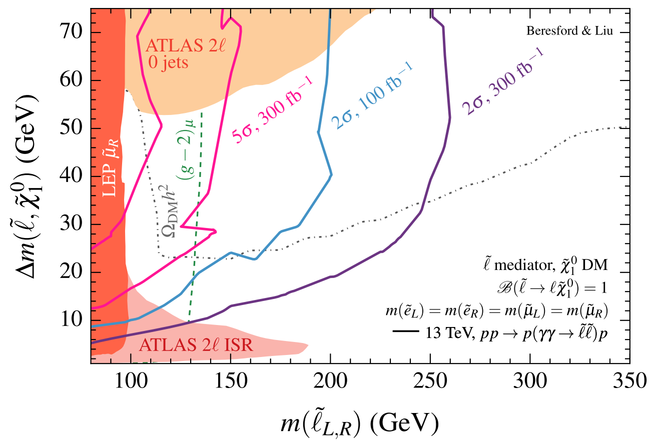

FIG. 3. Projected photon collider sensitivity of $\gamma\gamma \to \tilde{\ell}\tilde{\ell}$ using 13 TeV proton-tagged LHC collisions. Solid lines (this Letter) show the 2σ sensitivity contours for integrated luminosities of 100 fb^{-1} (blue) and 300 fb^{-1} (purple), along with 5σ at 300 fb^{-1} (pink). A simplified model of slepton mediators $\tilde{\ell}$ with a fourfold mass degeneracy decaying to neutralino DM $\tilde{\chi}_1^0$ is considered. Filled regions denote constraints from ATLAS 2ℓ 0 jets [11,12] (yellow), 2ℓ ISR searches [14] (pink), and LEP for partners of the right-handed muons $\tilde{\mu}_R$ [15–17] (orange). Dashed lines indicate parameter space favored by relic abundance $\Omega_{\text{DM}}h^2$ [4] (gray) and muon $(g-2)_\mu$ [8] (green) measurements, computed using MICROMEGAS [80].

Figure 3 shows the 2σ "sensitivity" contours of our search strategy (the solid lines) in the $\Delta m(\tilde{\ell}, \tilde{\chi}_1^0)$ vs $m(\tilde{\ell})$ plane, with 5σ "discovery" contours displayed for 300 fb^{-1}. For each signal point, we use the highest significance out of the three SRs. Our strategy unambiguously surpasses the existing collider sensitivity (the filled regions) in the $15 \lesssim \Delta m(\tilde{\ell}, \tilde{\chi}_1^0) \lesssim 60$ GeV corridor. For $\Delta m(\tilde{\ell}, \tilde{\chi}_1^0) \sim 40$ GeV, 2σ sensitivity reaches $m(\tilde{\ell}) \sim 200(250)$ GeV for $100\,(300)$ fb^{-1}, while 5σ sensitivity extends up to $m(\tilde{\ell}) \sim 140$ GeV using 300 fb^{-1}.

The mass reach depends on several factors. As $m(\tilde{\ell})$ increases, the $\gamma\gamma \to \tilde{\ell}\tilde{\ell}$ cross section decreases and the search becomes statistically limited. However, signals with larger $m(\tilde{\ell})$ are easier to distinguish from the WW background as the signal becomes better separated from the W boson mass; higher DM masses are similarly easier to separate. For $m(\tilde{\ell}) \lesssim 120$ GeV, sensitivity is limited by the forward detector acceptance.

The canonical LHC search for sleptons employs the "2ℓ 0 jets" signature, where the ATLAS 8 TeV, 20.3 fb^{-1} analysis gives the most stringent limit for $m(\tilde{\ell}) \lesssim 250$ GeV [11]. Notably, the 13 TeV, 36.1 fb^{-1} counterpart [12] did not surpass the 8 TeV analysis sensitivity for $\Delta m(\tilde{\ell}, \tilde{\chi}_1^0) \lesssim 60$ GeV, despite higher center-of-mass energy and luminosity, with similar results from CMS [13].

Our strategy has limited sensitivity to the compressed region $\Delta m(\tilde{\ell}, \tilde{\chi}_1^0) \lesssim 10$ GeV due to the trigger emulation

$p_T^\ell > 15$ GeV. Recent strategies propose initial state radiation (ISR) and low p_T leptons to probe this challenging region [81,82], as adopted by the ATLAS 2ℓ ISR search [14]. Our strategy could gain sensitivity here if lepton trigger thresholds are lowered by using AFP and CT-PPS information, motivating future developments.

A striking feature of Fig. 3 is that our proposal decisively probes regions favored by DM and muon $(g-2)_\mu$ phenomenology. We evaluate these noncollider observables using MICROMEGAS v4.2.1 [80]. The gray dashed contour indicates where the $\tilde{\chi}_1^0$ relic abundance matches the Planck measurement $\Omega_{\tilde{\chi}_1^0} h^2 = \Omega_{\rm DM}^{\rm Planck} h^2 = 0.12$ [4]. Depletion of $\Omega_{\tilde{\chi}_1^0} h^2$ occurs via coannihilation processes such as $\tilde{\ell}\tilde{\chi}_1^0 \to \ell\gamma$, whose rate grows exponentially $\sim e^{-\Delta m(\tilde{\ell},\tilde{\chi}_1^0)/m(\tilde{\ell})}$ with smaller mass differences [5,6]. At low $m(\tilde{\ell})$, the self-annihilation via the Z boson "funnel" becomes competitive, allowing larger mass splittings to satisfy $\Omega_{\rm DM}^{\rm Planck} h^2$. Loop corrections from $\tilde{\ell}$ and $\tilde{\chi}_1^0$ states contribute to the muon anomalous magnetic moment $a_\mu = \frac{1}{2}(g-2)_\mu$. The green dashed line indicates modifications consistent with the measured discrepancy $\Delta a_\mu = a_\mu^{\rm measured} - a_\mu^{\rm predicted} \simeq 2.5 \times 10^{-9}$ [8]. While we consider these features in a simplified model, the phenomenology is qualitatively consistent with those in global fits of more complete 11-parameter models [83].

If the fourfold mass degeneracy scheme is relaxed, the LHC blind corridor widens to $10 \lesssim \Delta m(\tilde{\mu}_R, \tilde{\chi}_1^0) \lesssim 90$ GeV [11–14], where our strategy will play an important role. In conventional electroweak production, the right-handed states $\tilde{\ell}_R$ have order 3 times smaller cross sections than the left-handed $\tilde{\ell}_L$ counterparts [84]. By contrast, the photon collider strategy has the advantage of equal QED cross sections for $\tilde{\ell}_L$ and $\tilde{\ell}_R$ states.

This proposal is widely extendable to other search channels and electrically charged targets. So-called R-parity violating scenarios where the $\tilde{\chi}_1^0$ decays to higher multiplicity final states can profit from clean events. Charged fermions (charginos) face similar difficulties discriminating against WW backgrounds and may benefit in combination with a hadronic channel. Scalar quarks, charged Higgs bosons, spin 1 mediators, and disappearing track signatures are also motivating scenarios.

In summary, we proposed a search strategy using the LHC as a photon collider to open sensitivity beyond LEP in the challenging corridor $15 \lesssim \Delta m(\tilde{\ell}, \tilde{\chi}_1^0) \lesssim 60$ GeV favored by DM and $(g-2)_\mu$ phenomenology. Proton tagging enables the initial state and missing momentum four-vector $p_{\rm miss}$ to be reconstructed, offering striking background discrimination inaccessible to current LHC searches. We encourage experimental collaborations to include this forward physics frontier in flagship hadron collider searches for DM and their charged mediators.

We thank the DM@LHC Workshop at Heidelberg University, where discussions for this work began, for the hospitality. We are grateful to Alan Barr for the helpful conversations and feedback on the manuscript. We also thank Jamie Boyd, Savannah Clawson, Till Eifert, Will Fawcett, Barak Gruberg, Lucian Harland-Lang, Valery Khoze, Tommaso Lari, Paul Newman, Christoph Paus, Andy Pilkington, Rafał Staszewski, and Marek Tasevsky for the useful discussions. L. B. is supported by St. John's College, Oxford. J. L. is supported by STFC.

[*]lydia.beresford@physics.ox.ac.uk
[†]jesse.liu@physics.ox.ac.uk

[1] H. Goldberg, Constraint on the Photino Mass from Cosmology, Phys. Rev. Lett. **50**, 1419 (1983); Erratum, Phys. Rev. Lett. **103**, 099905(E) (2009).

[2] J. R. Ellis, J. S. Hagelin, D. V. Nanopoulos, K. A. Olive, and M. Srednicki, Supersymmetric relics from the big bang, Nucl. Phys. **B238**, 453 (1984).

[3] G. Bertone, D. Hooper, and J. Silk, Particle dark matter: Evidence, candidates and constraints, Phys. Rep. **405**, 279 (2005).

[4] Planck Collaboration, Planck 2018 results. VI. Cosmological parameters, arXiv:1807.06209.

[5] K. Griest and D. Seckel, Three exceptions in the calculation of relic abundances, Phys. Rev. D **43**, 3191 (1991).

[6] J. Edsjo and P. Gondolo, Neutralino relic density including coannihilations, Phys. Rev. D **56**, 1879 (1997).

[7] Muon $g-2$ Collaboration, Final report of the muon E821 anomalous magnetic moment measurement at BNL, Phys. Rev. D **73**, 072003 (2006).

[8] T. Aoyama, M. Hayakawa, T. Kinoshita, and M. Nio, Complete Tenth-Order QED Contribution to the Muon $g-2$, Phys. Rev. Lett. **109**, 111808 (2012).

[9] K. Hagiwara, R. Liao, A. D. Martin, D. Nomura, and T. Teubner, $(g-2)_\mu$ and $\alpha(M_Z^2)$ re-evaluated using new precise data, J. Phys. G **38**, 085003 (2011).

[10] M. A. Ajaib, B. Dutta, T. Ghosh, I. Gogoladze, and Q. Shafi, Neutralinos and sleptons at the LHC in light of muon $(g-2)_\mu$, Phys. Rev. D **92**, 075033 (2015).

[11] ATLAS Collaboration, Search for direct production of charginos, neutralinos and sleptons in final states with two leptons and missing transverse momentum in pp collisions at $\sqrt{s} = 8$ TeV with the ATLAS detector, J. High Energy Phys. 05 (2014) 071.

[12] ATLAS Collaboration, Search for electroweak production of supersymmetric particles in final states with two or three leptons at $\sqrt{s} = 13$ TeV with the ATLAS detector, Eur. Phys. J. C **78**, 995 (2018).

[13] CMS Collaboration, Search for supersymmetric partners of electrons and muons in proton-proton collisions at $\sqrt{s} = 13$ TeV, Phys. Lett. B **790**, 140 (2019).

[14] ATLAS Collaboration, Search for electroweak production of supersymmetric states in scenarios with compressed mass spectra at $\sqrt{s} = 13$ TeV with the ATLAS detector, Phys. Rev. D **97**, 052010 (2018).

[15] ALEPH, DELPHI, L3, OPAL Experiments, Combined LEP Selectron/Smuon/Stau Results, 183–208 GeV, Technical Report No. LEPSUSYWG/04-01.1, 2004.
[16] ALEPH Collaboration, Search for scalar leptons in e^+e^- collisions at center-of-mass energies up to 209 GeV, Phys. Lett. B **526**, 206 (2002).
[17] L3 Collaboration, Search for scalar leptons and scalar quarks at LEP, Phys. Lett. B **580**, 37 (2004).
[18] F. del Aguila and L. Ametller, On the detectability of sleptons at large hadron colliders, Phys. Lett. B **261**, 326 (1991).
[19] H. Baer, C.-H. Chen, F. Paige, and X. Tata, Detecting sleptons at hadron colliders and supercolliders, Phys. Rev. D **49**, 3283 (1994).
[20] H. Baer, C.-H. Chen, F. Paige, and X. Tata, Signals for minimal supergravity at the CERN Large Hadron Collider. II. Multilepton channels, Phys. Rev. D **53**, 6241 (1996).
[21] J. Alwall, P. C. Schuster, and N. Toro, Simplified models for a first characterization of new physics at the LHC, Phys. Rev. D **79**, 075020 (2009).
[22] J. Alwall, M. P. Le, M. Lisanti, and J. G. Wacker, Model-independent jets plus missing energy searches, Phys. Rev. D **79**, 015005 (2009).
[23] D. Alves *et al.* (LHC New Physics Working Group), Simplified models for LHC new physics searches, J. Phys. G **39**, 105005 (2012).
[24] R. Essig, E. Izaguirre, J. Kaplan, and J. G. Wacker, Heavy flavor simplified models at the LHC, J. High Energy Phys. 01 (2012) 074.
[25] O. Buchmueller, M. J. Dolan, S. A. Malik, and C. McCabe, Characterising dark matter searches at colliders and direct detection experiments: Vector mediators, J. High Energy Phys. 01 (2015) 037.
[26] J. Abdallah *et al.*, Simplified models for dark matter searches at the LHC, Phys. Dark Universe **9–10**, 8 (2015).
[27] D. Abercrombie *et al.*, Dark matter benchmark models for early LHC run-2 searches: Report of the ATLAS/CMS Dark Matter Forum, arXiv:1507.00966.
[28] ATLAS Collaboration, Search for dark matter and other new phenomena in events with an energetic jet and large missing transverse momentum using the ATLAS detector, J. High Energy Phys. 01 (2018) 126.
[29] ATLAS Collaboration, Search for new phenomena in dijet mass and angular distributions from pp collisions at $\sqrt{s} =$ 13 TeV with the ATLAS detector, Phys. Lett. B **754**, 302 (2016).
[30] ATLAS Collaboration, Search for dark matter at $\sqrt{s} =$ 13 TeV in final states containing an energetic photon and large missing transverse momentum with the ATLAS detector, Eur. Phys. J. C **77**, 393 (2017).
[31] ATLAS Collaboration, Search for Dark Matter Produced in Association with a Higgs Boson Decaying to $b\bar{b}$ using 36 fb^{-1} of pp Collisions at $\sqrt{s} = 13$ TeV with the ATLAS Detector, Phys. Rev. Lett. **119**, 181804 (2017).
[32] B. Dutta, K. Fantahun, A. Fernando, T. Ghosh, J. Kumar, P. Sandick, P. Stengel, and J. W. Walker, Probing squeezed bino-slepton spectra with the Large Hadron Collider, Phys. Rev. D **96**, 075037 (2017).
[33] K. Piotrzkowski, Tagging two photon production at the CERN LHC, Phys. Rev. D **63**, 071502(R) (2001).
[34] ATLAS Collaboration, Technical design report for the ATLAS Forward Proton detector, Technical Reports No. CERN-LHCC-2015-009 and No. ATLAS-TDR-024, 2015.
[35] M. Albrow *et al.* (CMS and TOTEM diffractive and Forward Physics Working Group), Prospects for diffractive and forward physics at the LHC, Technical Report No. CERN-LHCC-2006-039-G-124.
[36] CMS and TOTEM Collaborations, CMS-TOTEM precision proton spectrometer technical design report, Technical Report No. CERN-LHCC-2014-021, TOTEM-TDR-003, CMS-TDR-13, 2014.
[37] CMS and TOTEM Collaborations, Observation of proton-tagged, central (semi)exclusive production of high-mass lepton pairs in pp collisions at 13 TeV with the CMS-TOTEM precision proton spectrometer, J. High Energy Phys. 07 (2018) 153.
[38] D. d'Enterria and G. G. da Silveira, Observing Light-By-Light Scattering at the Large Hadron Collider, Phys. Rev. Lett. **111**, 080405 (2013); Erratum, Phys. Rev. Lett. **116**, 129901(E) (2016).
[39] ATLAS Collaboration, Evidence for light-by-light scattering in heavy-ion collisions with the ATLAS detector at the LHC, Nat. Phys. **13**, 852 (2017).
[40] E. Chapon, C. Royon, and O. Kepka, Anomalous quartic $WW\gamma\gamma$, $ZZ\gamma\gamma$, and trilinear $WW\gamma$ couplings in two-photon processes at high luminosity at the LHC, Phys. Rev. D **81**, 074003 (2010).
[41] S. Fichet, G. von Gersdorff, O. Kepka, B. Lenzi, C. Royon, and M. Saimpert, Probing new physics in diphoton production with proton tagging at the Large Hadron Collider, Phys. Rev. D **89**, 114004 (2014).
[42] S. Knapen, T. Lin, H. K. Lou, and T. Melia, Searching for Axionlike Particles with Ultraperipheral Heavy-Ion Collisions, Phys. Rev. Lett. **118**, 171801 (2017).
[43] C. Baldenegro, S. Fichet, G. von Gersdorff, and C. Royon, Searching for axion-like particles with proton tagging at the LHC, J. High Energy Phys. 06 (2018) 131.
[44] Sylvain Fichet, Shining light on polarizable dark particles, J. High Energy Phys. 04 (**2017**) 088.
[45] V. A. Khoze, A. D. Martin, and M. G. Ryskin, Can invisible objects be seen via forward proton detectors at the LHC?, J. Phys. G **44**, 055002 (2017).
[46] J. Ohnemus, T. F. Walsh, and P. M. Zerwas, $\gamma\gamma$ production of non-strongly interacting SUSY particles at hadron colliders, Phys. Lett. B **328**, 369 (1994).
[47] N. Schul and K. Piotrzkowski, Detection of two-photon exclusive production of supersymmetric pairs at the LHC, Nucl. Phys. B, Proc. Suppl. **179–180**, 289 (2008).
[48] FP420 R & D Collaboration, The FP420 R & D Project: Higgs and new physics with forward protons at the LHC, J. Instrum. **4**, T10001 (2009).
[49] J. de Favereau de Jeneret, V. Lemaitre, Y. Liu, S. Ovyn, T. Pierzchala, K. Piotrzkowski, X. Rouby, N. Schul, and M. Vander Donckt, High energy photon interactions at the LHC, arXiv:0908.2020.
[50] L. A. Harland-Lang, C. H. Kom, K. Sakurai, and W. J. Stirling, Measuring the masses of a pair of semi-invisibly decaying particles in central exclusive production with forward proton tagging, Eur. Phys. J. C **72**, 1969 (2012).

[51] V. M. Budnev, I. F. Ginzburg, G. V. Meledin, and V. G. Serbo, The two photon particle production mechanism. Physical problems. Applications. Equivalent photon approximation, Phys. Rep. **15**, 181 (1975).

[52] S. J. Brodsky, T. Kinoshita, and H. Terazawa, Two photon mechanism of particle production by high-energy colliding beams, Phys. Rev. D **4**, 1532 (1971).

[53] G. Tupper and M. A. Samuel, W^+W^- pair production in two-photon collisions and the magnetic moment of the $W^\pm$ bosons, Phys. Rev. D **23**, 1933 (1981).

[54] J. Alwall, M. Herquet, F. Maltoni, O. Mattelaer, and T. Stelzer, MadGraph 5: Going beyond, J. High Energy Phys. 06 (2011) 128.

[55] J. Alwall, R. Frederix, S. Frixione, V. Hirschi, F. Maltoni, O. Mattelaer, H.-S. Shao, T. Stelzer, P. Torrielli, and M. Zaro, The automated computation of tree-level and next-to-leading order differential cross sections, and their matching to parton shower simulations, J. High Energy Phys. 07 (2014) 079.

[56] L. Heinrich, LUKASHEINRICH/PYLHE v0.0.4, https://doi.org//10.5281/zenodo.1217032, 2018.

[57] See Supplemental Material at http://link.aps.org/supplemental/10.1103/PhysRevLett.123.141801 for details of selection efficiency, soft survival probabilities, forward detector acceptance, and pileup mitigation strategies.

[58] V. A. Khoze, A. D. Martin, and M. G. Ryskin, Prospects for new physics observations in diffractive processes at the LHC and tevatron, Eur. Phys. J. C **23**, 311 (2002).

[59] V. A. Khoze, A. D. Martin, and M. G. Ryskin, Diffraction at the LHC, Eur. Phys. J. C **73**, 2503 (2013).

[60] L. A. Harland-Lang, V. A. Khoze, and M. G. Ryskin, Exclusive LHC physics with heavy ions: SuperChic 3, Eur. Phys. J. C **79**, 39 (2019).

[61] ATLAS Collaboration, Studies of the performance of the ATLAS detector using cosmic-ray muons, Eur. Phys. J. C **71**, 1593 (2011).

[62] J. de Favereau, C. Delaere, P. Demin, A. Giammanco, V. Lematre, A. Mertens, and M. Selvaggi (DELPHES 3 Collaboration), DELPHES 3, A modular framework for fast simulation of a generic collider experiment, J. High Energy Phys. 02 (2014) 057.

[63] A. J. Barr, Measuring slepton spin at the LHC, J. High Energy Phys. 02 (2006) 042.

[64] T. Melia, Spin before mass at the LHC, J. High Energy Phys. 01 (2012) 143.

[65] C. G. Lester and D. J. Summers, Measuring masses of semi-invisibly decaying particles pair produced at hadron colliders, Phys. Lett. B **463**, 99 (1999).

[66] A. Barr, C. Lester, and P. Stephens, A variable for measuring masses at hadron colliders when missing energy is expected; m_{T2}: The truth behind the glamour, J. Phys. G **29**, 2343 (2003).

[67] C. G. Lester and B. Nachman, Bisection-based asymmetric M_{T2} computation: A higher precision calculator than existing symmetric methods, J. High Energy Phys. 03 (2015) 100.

[68] ATLAS Collaboration, Measurement of the exclusive $\gamma\gamma \to \mu^+\mu^-$ process in proton-proton collisions at $\sqrt{s} =$ 13 TeV with the ATLAS detector, Phys. Lett. B **777**, 303 (2018).

[69] ATLAS Collaboration, Measurement of exclusive $\gamma\gamma \to W^+W^-$ production and search for exclusive Higgs boson production in pp collisions at $\sqrt{s} = 8$ TeV using the ATLAS detector, Phys. Rev. D **94**, 032011 (2016).

[70] CMS Collaboration, Evidence for exclusive $\gamma\gamma \to W^+W^-$ production and constraints on anomalous quartic gauge couplings in pp collisions at $\sqrt{s} = 7$ and 8 TeV, J. High Energy Phys. 08 (2016) 119.

[71] ATLAS Collaboration, Zero degree calorimeters for ATLAS, Technical Report No. CERN-LHCC-2007-01, 2007.

[72] M. W. Phipps, A new ATLAS ZDC for the high radiation environment at the LHC, Technical Report No. ATL-FWD-SLIDE-2018-288, 2018.

[73] C. Royon, M. Saimpert, O. Kepka, and R. Zlebcik, Timing detectors for proton tagging at the LHC, Acta Phys. Pol. B **7**, 735 (2014).

[74] L. Bonnet, J. Liao, and K. Piotrzkowski, Study on GASTOF A 10 ps resolution timing detector, Nucl. Instrum. Methods Phys. Res., Sect. A **762**, 77 (2014).

[75] L. A. Harland-Lang, V. A. Khoze, M. G. Ryskin, and M. Tasevsky, LHC searches for dark matter in compressed mass scenarios: Challenges in the forward proton mode, J. High Energy Phys. 04 (2019) 010.

[76] R. Staszewski and J. Chwastowski, Timing detectors for forward physics, Nucl. Instrum. Methods Phys. Res., Sect. A **940**, 45 (2019).

[77] ATLAS Collaboration, Prospects and results from the AFP detector in ATLAS, Report No. ATL-FWD-SLIDE-2019-165, 2019.

[78] G. Cowan, Discovery sensitivity for a counting experiment with background uncertainty, www.pp.rhul.ac.uk/ cowan/stat/medsig/medsigNote.pdf.

[79] G. Cowan, K. Cranmer, E. Gross, and O. Vitells, Asymptotic formulae for likelihood-based tests of new physics, Eur. Phys. J. C **71**, 1554 (2011); Erratum, Eur. Phys. J. C **73**, 2501(E) (2013).

[80] G. Blanger, F. Boudjema, A. Pukhov, and A. Semenov, MICROMEGAs 4.1: Two dark matter candidates, Comput. Phys. Commun. **192**, 322 (2015).

[81] Z. Han and Y. Liu, M_{T2} to the rescue: Searching for sleptons in compressed spectra at the LHC, Phys. Rev. D **92**, 015010 (2015).

[82] A. Barr and J. Scoville, A boost for the EW SUSY hunt: Monojet-like search for compressed sleptons at LHC14 with 100 fb^1, J. High Energy Phys. 04 (2015) 147.

[83] E. Bagnaschi *et al.*, Likelihood analysis of the pMSSM11 in light of LHC 13-TeV data, Eur. Phys. J. C **78**, 256 (2018).

[84] B. Fuks, M. Klasen, D. R. Lamprea, and M. Rothering, Revisiting slepton pair production at the Large Hadron Collider, J. High Energy Phys. 01 (2014) 168.